The Iraqi Journal For Mechanical And Material Engineering, Vol.9, No.1, 2009

PREDICTION OF SHOCK WAVE AND EXTERNAL FLOW FIELD PARAMETERS IN A MODERATE SUPERSONIC FLOW OVER A 3-D ARC CIRCULAR BUMP

Dr. Ahmed Kadhim Hussein
*Babylon University / Eng. College / Mech. Eng. Dept –Hilla Iraq

ABSTRACT

This study is used to compute the primitive variables of moderate supersonic flow based on finite difference computational fluid dynamic methods. The problem considered deals with a three-dimensional external, inviscid ,compressible supersonic flow over a three-dimensional arc circular bump. In this work, Euler equation was solved using time-marching MacCormack's explicit technique. The flow conditions are taken at sea level and Mach number at **1.97**. To deal with complex shape of arc circular bump the so-called "body fitted coordinate system" were considered and the algebraic methods were used to generate grids over an arc circular bump. The results showed a good agreement with other published results.

.الخلاصة:

في هذا البحث تم إظهار أهمية الحل العددي في أيجاد حل للمشاكل الأيروديناميكية عند السرع الصوتية العالية المعتدلة أي (**supersonic flow**) عندما يكون رقم ماخ اعلى من واحد. تم اللجوء الى الأسلوب العددي لتعذر حل المشكلة الهندسية تحليلياً وكذلك فأن حل أي مشكلة أيروديناميكية تحتاج الى نفق هوائي (**supersonic wind tunnel**) وهو غير متوفر في العراق ويتطلب وقت زمني كبير جداً لاجراء التجارب. في الدراسة الحالية تم التعامل مع برنامج هندسي متكامل وتطويره للتعامل مع الجريان فوق الصوتي وإيجاد المتغيرات الأساسية (**primitive variables**) وهي السرعة والضغط ودرجة الحرارة والكثافة ورقم ماخ والطاقة الداخلية عند أي نقطة . تضمن أسلوب الحل ، حل معادلة أويلر وتم توليد مجاميع النقاط بواسطة تقنية (**mesh generation**) وتم أختيار **arc circular bump** كحالة للدراسة. الحل العددي تم بأستخدام طريقة ماكارموك(MacCormack's Method) وهي طريقة كفوءه عند استخدامها لدراسة الجريان الخارجي فوق الصوتي وتم اختيار رقم ماخ للجريان الخارجي (Free stream Mach number) بقيمة(**1.97**) كحالة دراسة وايضاً تم دراسة تأثير موجات الصدمة (**shock waves**) على حساب المتغيرات الأساسية للجريان الخارجي الانضغاطي وباهمال تاثير لزوجة الجريان.

Keyword: Arc circular bump , CFD, Supersonic aerodynamics, Euler equation.

finite difference method with time marching was adopted to predict the aerodynamic characteristics of three-dimensional external compressible inviscid supersonic flow over an arc circular bump to compute the primitive variables such as the internal energy, pressure, density, Mach number and temperature at each grid. The time-marching method was chosen to treat an arc circular bump as a plane body. In the next section, the mathematical analysis will be described in detail and the style, which used to produce meshes or grids are given. It is very important to refer that the primitive variable covers, velocity, density, temperature, pressure, internal energy and Mach number.

Mathematical Analysis

The studied supersonic flow is a non-viscous, non-heat conducting fluid, so it is described by Euler equation. The latter is obtained from Navier-Stokes equations by neglecting all shear stresses and heat-conduction terms, so it is a valid approximation for flows at high speed (supersonic flow), i.e., at high Reynolds number outside the viscous region developing near the solid surface. The mathematical behavior of the Euler equation is classified as hyperbolic in supersonic flow Hosseini (2006). The solution is obtained using time-marching method. In this method two points must be noticed.

1. The grid points are generated in physical plane and transformed to computational plane before solving governing equations.
2. The solution is obtained by marching from some initial flow field through time until a steady – state is obtained.

The governing equations for an inviscid, non-heat conducting, external, compressible, three-dimensional supersonic flow expressed in conservation form are Hoffmann (1989):

Continuity equation:

$$\nabla.(\rho V)=\frac{\partial \rho}{\partial t}+\frac{\partial(\rho u)}{\partial x}+\frac{\partial(\rho v)}{\partial y}+\frac{\partial(\rho w)}{\partial z} \qquad \textbf{(1)}$$

The conservation of momentum equation is :

$$\frac{\partial(\rho u)}{\partial t}+\frac{\partial(\rho u^2+p)}{\partial x}+\frac{\partial(\rho u v)}{\partial y}+\frac{\partial(\rho u w)}{\partial z}=0$$

$$\frac{\partial(\rho v)}{\partial t}+\frac{\partial(\rho u v)}{\partial x}+\frac{\partial(\rho v^2+p)}{\partial y}+\frac{\partial(\rho v w)}{\partial z}=0$$

$$\frac{\partial(\rho w)}{\partial t}+\frac{\partial(\rho u w)}{\partial x}+\frac{\partial(\rho w v)}{\partial y}+\frac{\partial(\rho w^2+p)}{\partial z}=0 \qquad \textbf{(2)}$$

The conservation of energy equation is :

$$\frac{\partial(\rho E_t)}{\partial t}+\frac{\partial}{\partial x}[(\rho E_t+p)u]+\frac{\partial}{\partial y}[(\rho E_t+p)v]+\frac{\partial}{\partial z}[(\rho E_t+p)w]=0 \qquad \textbf{(3)}$$

It is suitable to put these equations in a vector form before applying a numerical scheme to these equations. The 3-dimensinal Euler equation may be arranged in a vector form as Hoffmann (1989)

$$\frac{\partial Q}{\partial t}+\frac{\partial E}{\partial x}+\frac{\partial F}{\partial y}+\frac{\partial G}{\partial z}=0 \qquad \textbf{(4)}$$

where Q,E,F and G are column vectors which is defined by:

$$Q=\frac{\partial}{\partial t}=\begin{bmatrix}\rho\\ \rho u\\ \rho \upsilon\\ \rho E_t\end{bmatrix};\ E=\frac{\partial}{\partial x}=\begin{bmatrix}\rho u\\ \rho u^2+P\\ \rho u\upsilon\\ (\rho E_t+P)u\end{bmatrix};\ F=\frac{\partial}{\partial y}=\begin{bmatrix}\rho \upsilon\\ \rho u\upsilon\\ \rho \upsilon^2+P\\ (\rho E_t+P)\upsilon\end{bmatrix};$$

$$G=\frac{\partial}{\partial z}=\begin{bmatrix}\rho w\\ \rho uw\\ \rho w^2+P\\ (\rho E_t+P)w\end{bmatrix} \qquad \textbf{(5)}$$

also the equation of state is given by :-

$p=\rho RT$, at ambient temperature, it becomes :-

$$\rho_\infty=\frac{p_\infty}{RT_\infty} \qquad \textbf{(6)}$$

and the speed of sound is given by :-

$$a_\infty=\sqrt{\gamma RT_\infty}$$

The total pressure and temperature (or stagnation pressure and temperature) are given by: -

$$p_o=p_\infty\left[1+\frac{(\gamma-1)}{2}M^2\right]^{\frac{\gamma}{\gamma-1}} \qquad \textbf{(7)}$$

$$T_o=T_\infty\left[1+\frac{(\gamma-1)}{2}M^2\right] \qquad \textbf{(8)}$$

The Reynolds number and boundary layer thickness are given by :-

$$\mathrm{Re}=\frac{\rho_\infty u_\infty L}{\mu_\infty} \qquad \text{and } \delta=\frac{5.0L}{\mathrm{Re}_L^{0.5}} \qquad \textbf{(9)}$$

Moreover the velocity components are given by :-

$$u_\infty=V\cos\alpha \qquad \textbf{(10-A)}$$

$$\upsilon_\infty=V\sin\alpha \qquad \textbf{(10-B)}$$

where $V = M\, a_\infty$ noting that:-

M=Mach number. and a_∞ = speed of sound.

V =Fluid velocity.

δ =Boundary layer thickness.

Re=Reynolds number.

μ_∞ =Free stream dynamic viscosity.

Three- Dimensional Mesh Generation:

In this work, the algebraic grid generation method is used to produce mesh. This method generates grid points in space by means of interpolations based on given boundary data. Because of the non-uniform shape of arc circular bump, a " body-fitted coordinate system " is used which enable us for the transformation of governing equations from a Cartesian system **(x ,y,z)** to a general curvilinear system **(ζ,η,ξ)** and it help us to transform from physical plane to the computational plane Fox (1993).The transformation of any partial differential equations from physical plane (x, y,z) to computational plane (ζ,η,ξ) are defined by the following relations :-

$$\xi = \xi(x,y,z) \tag{11-A}$$

$$\zeta = \zeta(x,y,z) \tag{11-B}$$

$$\eta = \eta(x,y,z) \tag{11-C}$$

The details of transformation is very long and complex, for more details, it is recommended to see Hoffmann (1989) and the results are given by:

$$J = \frac{1}{x_\xi\left[y_\eta z_\zeta - z_\eta y_\zeta\right] - x_\eta\left[y_\xi z_\zeta - z_\xi y_\zeta\right] + x_\zeta\left[y_\xi z_\eta - z_\xi y_\eta\right]} \tag{12}$$

where J is the jacobian of transformation, and it is defined as the ratio of the volumes in the physical space to that of the computational space. Also the metrics of transformation are given (in 3-D domain) as follows:-

$$\begin{aligned} \xi_x &= J\left[y_\eta z_\zeta - y_\zeta z_\eta\right] & \eta_x &= -J\left[y_\xi z_\zeta - y_\zeta z_\xi\right] \\ \xi_y &= -J\left[x_\eta z_\zeta - x_\zeta z_\eta\right] & \eta_y &= J\left[x_\xi z_\zeta - x_\zeta z_\xi\right] \\ \xi_z &= J\left[x_\eta y_\zeta - x_\zeta y_\eta\right] & \eta_z &= -J\left[x_\xi y_\zeta - x_\zeta y_\xi\right] \end{aligned} \tag{13-A}$$

and

$$\begin{aligned} \zeta_x &= J\left[y_\xi z_\eta - y_\eta z_\xi\right] \\ \zeta_y &= -J\left[x_\xi z_\eta - x_\eta z_\xi\right] \\ \zeta_z &= -J\left[x_\xi y_\eta - x_\eta y_\xi\right] \end{aligned} \tag{13-B}$$

the physical meaning of the metrics is that, it represents the ratio of arc length in the computational space to that of the physical space. The terms x_ζ , x_η , y_ζ …. are computed numerically using forward approximation, as an example :-

$$y_\eta = \frac{\partial y}{\partial \eta} = \frac{-3y_{i,j,k} + 4y_{i,j+1,k} - y_{i,j+2,k}}{2\Delta\eta} \qquad \textbf{(14)}$$

Numerical Scheme:

Explicit time-dependent solution of the three-dimensional Euler equations has been performed using MacCormack's predictor-corrector finite difference technique, which is second-order accurate in both space and time. This method is very effective finite difference technique for viscous and inviscid supersonic flow, specially for unsteady flow shock capturing. By using this technique a computer code is constructed to predict the shock wave which consists from the following steps:

1. a three-dimensional domain is chosen over a arc circular bump, which consists from (im=21, jm=16 and km=21), where:-

im = maximum number of grids in x-direction.
jm = maximum number of grids in y-direction.
km = maximum number of grids in z-direction.

2. a grid generation is performed in (**x-y-z)** direction and the Jacobian and different metrics are calculated.
3. a flow conditions such as (u,v,w,M,T, e, ρ and P) are computed at the surface (k=1) and then they are computed in the domain except at the surface where (I=1 to I=im, j=1 to j=jm, k=2 to k=km).
4. a time step calculation is performed, the time step employed in this work is designed so that it is not exceed the maximum step size permitted by stability. In this study the inviscid CFL conditions AL-Dulaimy (2002) is used which is given by the following relation: -

$$\Delta t)_{CFL} \le \left[\frac{|u|}{\Delta x} + \frac{|\upsilon|}{\Delta y} + \frac{|w|}{\Delta z} + a * \left[\frac{1}{(\Delta x)^2} + \frac{1}{(\Delta y)^2} + \frac{1}{(\Delta z)^2} \right]^{\frac{1}{2}} \right]^{-1} \qquad (15)$$

5. a changing of primitive variables to fluxes is occurred which causes to compute the values of flux vectors for all grid points at time step (n).
6. a forward predictor version of MacCormack's which is given by Hoffmann (1989):-

$$\overline{Q}_{i,j,k}^{n+1} = \overline{Q}_{i,j,k}^{n} - \frac{\Delta t}{\Delta \xi}\left[\overline{E}_{i+1,j,k}^{n+1} - \overline{E}_{i,j,k}^{n+1}\right] - \frac{\Delta t}{\Delta \eta}\left[\overline{F}_{i,j+1,k}^{n+1} - \overline{F}_{i,j,k}^{n+1}\right] - \frac{\Delta t}{\Delta \zeta}\left[G_{i,j,k+1}^{n+1} - G_{i,j,k}^{n+1}\right] \quad (16)$$

is used inside the domain where (I=2 to im-1, j=2 to jm-1, k=2 to km-1) where :-
n is the time level (t) and n+1 is the time level (t+dt).

7. In order to make our numerical scheme accurate and stable, since we deal with high velocities (high Reynolds number) the following expression for explicit artificial dissipation is added to the predictor step, where $SQ_{i,j,k}^{n+1}$ is a fourth-order artificial viscosity term, defined by Anderson (1995):-

$$SQ^{n+1}_{i,j,k} = C_\xi \frac{\left|P^n_{i-1,j,k} - 2P^n_{i,j,k} + P^n_{i-1,j,k}\right|}{P^n_{i-1,j,k} + 2P^n_{i,j,k} + P^n_{i-1,j,k}} * \left[Q_1^-\right)^n_{i-1,j,k} - 2Q_1^-\right)^n_{i,j,k} + Q_1^-\right)^n_{i+1,j,k}\Big]+$$

$$C_\eta \frac{\left|P^n_{i,j-1,k} - 2P^n_{i,j,k} + P^n_{i,j+1,k}\right|}{P^n_{i,j-1,k} + 2P^n_{i,j,k} + P^n_{i,j+1,k}} * \left[Q_1^-\right)^n_{i,j-1,k} - 2Q_1^-\right)^n_{i,j,k} + Q_1^-\right)^n_{i,j+1,k}\Big] \qquad (17)$$

$$+ C_\zeta \frac{\left|P^n_{i,j,k-1} - 2P^n_{i,j,k} + P^n_{i,j,k+1}\right|}{P^n_{i,j,k-1} + 2P^n_{i,j,k} + P^n_{i,j,k+1}} * \left[Q_1^-\right)^n_{i,j,k-1} - 2Q_1^-\right)^n_{i,j,k} + Q_1^-\right)^n_{i,j,k+1}\Big]$$

The main advantage of artificial dissipation is to provide some mathematical dissipation analogous to the real viscous effects inside the shock wave.

8. A decoding is occurred which is used to produce our parameters from fluxes, also at this step, the contravarient velocity components are computed as :-

$$\mathrm{U} = \xi_x u + \xi_y \upsilon + \xi_z \omega$$
$$\mathrm{V} = \eta_x u + \eta_y \upsilon + \eta_z w \qquad (18)$$
$$\mathrm{W} = \zeta_x u + \zeta_y \upsilon + \zeta_z w$$

are computed .The contravarient velocity components U,V and W represent velocity components which are perpendicular to planes of constant ξ, η and ζ

9. A corrector step is computed, where the value of fluxes (E ,F,G) are computed at each grid in the intermediate level (n+1) depending on the values of primitive variables from previous step, so the computations occurs inside the domain [i=1 to i=im, j=1 to j=jm and k=1 to k=km].
10. a backward corrector version of MacCormack's method which is given by Fox (1993) is then applied :-

$$Q^{n+1}_{i,j,k} = (1/2) * \left\{ \begin{array}{l} Q^n_{i,j,k} + \overline{Q}^{n+1}_{i,j,k} - \dfrac{\Delta t}{\Delta \xi}\left[\overline{E}^{n+1}_{i,j,k} - \overline{E}^{n+1}_{i,j-1,k}\right] \\ - \dfrac{\Delta t}{\Delta \eta}\left[\overline{F}^{n+1}_{i,j,k} - \overline{F}^{n+1}_{i,j-1,k}\right] - \dfrac{\Delta t}{\Delta \zeta}\left[G^{n+1}_{i,j,k} - G^{n+1}_{i,j-1,k}\right] \end{array} \right\} \qquad (19)$$

which is used inside the domain (i=2 to im-1, j=2 to jm-1, k=2 to km-1)and, also a fourth-order artificial viscosity term Anderson (1995) at corrector step is added to Eq.(19). This expression is given by:

$$SQ^{n+1}\Big)_{i,j,k} = C_\xi \frac{\left|P^{n+1}_{i+1,j,k} - 2P^{n+1}_{i,j,k} + P^{n+1}_{i-1,j,k}\right|}{\left[P^{n+1}_{i+1,j,k} - 2P^{n+1}_{i,j,k} + P^{n+1}_{i-1,j,k}\right]} * \left[\overline{Q}_1\right)^{n+1}_{i-1,j,k} - 2\overline{Q}_1\right)^{n+1}_{i,j,k} + \overline{Q}_1\right)^{n+1}_{i+1,j,k}\Big]+$$

$$C_\eta \frac{\left|P^{n+1}_{i,j+1,k} - 2P^{n+1}_{i,j,k} + P^{n+1}_{i,j-1,k}\right|}{\left[P^{n+1}_{i,j+1,k} - 2P^{n+1}_{i,j,k} + P^{n+1}_{i,j-1,k}\right]} * \left[\overline{Q}_1\right)^{n+1}_{i,j-1,k} - 2\overline{Q}_1\right)^{n+1}_{i,j,k} + \overline{Q}_1\right)^{n+1}_{i,j+1,k}\Big] \qquad (20)$$

$$+ C_\zeta \frac{\left|P^{n+1}_{i,j,k+1} - 2P^{n+1}_{i,j,k} + P^{n+1}_{i,j,k-1}\right|}{\left[P^{n+1}_{i,j,k+1} - 2P^{n+1}_{i,j,k} + P^{n+1}_{i,j,k-1}\right]} * \left[\overline{Q}_1\right)^{n+1}_{i,j,k-1} - 2\overline{Q}_1\right)^{n+1}_{i,j,k} + \overline{Q}_1\right)^{n+1}_{i,j,k+1}\Big]$$

11. after a corrector step is completed, a decoding step began where our parameters such as (u,v,w,P,T,e and M) are computed.

12. our parameters are computed under different boundary conditions which can be explained as follows:-
    a. up-stream boundary condition(i=1, j=1 to jm, k=1 to km) and at the edge of the body (k=1,i=1, j=1 to jm).

b. solid boundary condition (k=1,i=2 to im ,j=1 to jm)
c. down stream boundary condition (i=im, j=2 to jm-1 and k=2 to km-1).
d. upper plane of symmetry(j=jm, i=2 to im and k=2 to km).
e. plane of symmetry (j =jm, i=2 to im, k=2 to km).
f. far-field boundary condition (k=km, i=1 to im, j=1 to jm).

13.Examining solution convergence, knowing that the last flow field variable to be convergence is the density, therefore, the following convergence criterion was applied at every point in the flow field from one time step to the next Wylie (1966) :

$$\text{error} = \frac{\rho_{\text{old}} - \rho_{new}}{\rho_{old}} \leq 1*10^{-8} \qquad (21)$$

RESULTS AND DISCUSSION

Fig. (1) shows a mesh generation over a three-dimensional arc circular bump in a moderate supersonic compressible external inviscid flow. The mesh points are produced by using an algebraic grid generation with (21 x 16 x 21) grid points . The explicit technique has required about (4000) time steps to achieve the converged solution (steady state solution).In the present work, the artificial viscosity is taken as (0.5),as shown in the figure.

Fig. (2) shows a Mach number contours for 3D arc circular bump for free stream Mach number = 1.97. The shock wave can be noticed clearly. From this figure, the flow pattern near the leading edge of arc circular bump, where the incoming supersonic flow undergoing a sudden change in flow direction resulting a continuous compression wave. The angle of the shock wave depends on arc circular bump shape and free stream Mach number. The shock wave is observed to be detached from circular bump angle and flow behind the shock near the trailing edge of arc circular bump area becomes subsonic. Also, its very important to refer that the clustering process is very necessary near the leading edge of arc circular bump in order to capture all the expected shock waves. This prediction gives a good agreement with the experimental results dealing with the same problem as indicated in Marsden (2004).It is very useful to note that the predicted shock wave by the numerical solution of the current work decelerate the flow speed from supersonic speed up stream of the shock wave to subsonic flow down stream of the shock wave.

Fig. (3) shows a temperature contours for supersonic arc circular bump for free stream Mach number =1.97.This figure indicates that the temperature distribution occurs at the region between the arc circular bump surface and the shock wave. Also, the temperature increases at the leading edge of arc circular bump due to shock wave strength and is decreased gradually toward its free stream value. The higher temperature can be noticed at the edge of three-dimensional arc circular bump, due to shock wave effect.

Fig. (4) shows a pressure contours over a three-dimensional arc circular bump for free stream Mach number =1.97. From this figure, the pressure values increases a head of shock wave and then decreased toward its free stream value away from the shock wave. This is agree with Sorensen (2002) and Dietz (2004) also, the pressure

values is increased dramatically near the leading edge of arc circular bump due to shock wave effects.

Fig. (5) shows a density contours over a three-dimensional arc circular bump for free stream Mach number =1.97. From this figure, the density values increases due to increase of the pressure and this is due to increase in shock wave strength.

Fig. (6) shows the internal energy contours over a three-dimensional arc circular bump for free stream Mach number =1.97. This figure shows clearly the shock wave prediction and again the internal energy values increases due to shock wave effect. This behavior can be explained as follows:- Since the shock wave decelerate the flow from supersonic speed ahead of the shock wave to subsonic speed down stream of the shock wave. This is certainly causes a reduction in kinetic energy, due to direct proportionality between the flow speed and the kinetic energy and as a result causes an increase in internal energy.

Fig.s (7) and (8) explain the wall pressure profile along an arc circular bump and the historical convergence of numerical simulation of the same problem. The latter figure explains the intermediate solutions of time-dependent schemes. The time level (n=1) is the specified initial condition and the figure refers, that at iteration equals (4000) the steady state solution is reached. Obviously, this figure just explains a means of reaching to the steady state solution. However, if correct (from physical point of view) and accurate initial data is provided, the solution at various time levels will represent the time dependent solution and it is usually referred to as the time-accurate solution.

CONCLUSIONS

The following conclusions can be drawn from the results of the present work :-

1. a solution of Euler equation for three-dimensional arc circular bump converges at a range of (4000) iterations. The range of iteration is related to the procedure of grid producing.
2. for capturing the flow field parameters ; a more mesh points are required near the surface of the arc circular bump.
3. geometry and arc circular bump curvatures have an important effect on the flow field pattern; where in the supersonic flow the change in flow direction due to geometry induced a type of drag. This is called wave drag.
4. since the mesh generation has been separated from explicit solver any mesh type can be used. The stability of the solution depends on the number of grid points and CFL condition.
5. the rise in the value of temperature at the stagnation point is due to flow nature change from supersonic a head of the shock wave to subsonic down stream of the shock wave. This change will reduce the kinetic energy and at the same time, this reduction gives an increase in internal energy and as a result increase the temperature.
6. the time-marching solution which is used to deal with a three-dimensional arc circular bump, which can be extended to deal with an axis-symmetry body such as aircraft.
7. from the results obtained, the hydrodynamic properties such as pressure, temperature and density are increased due to shock wave effect
8. the software developed explains, that the convergence depends on the optimum values of the grid points, artificial viscosity and CFL.

9. clustering process is very necessary at the leading edge of the three-dimensional arc circular bump in order to capture the expected shock wave.

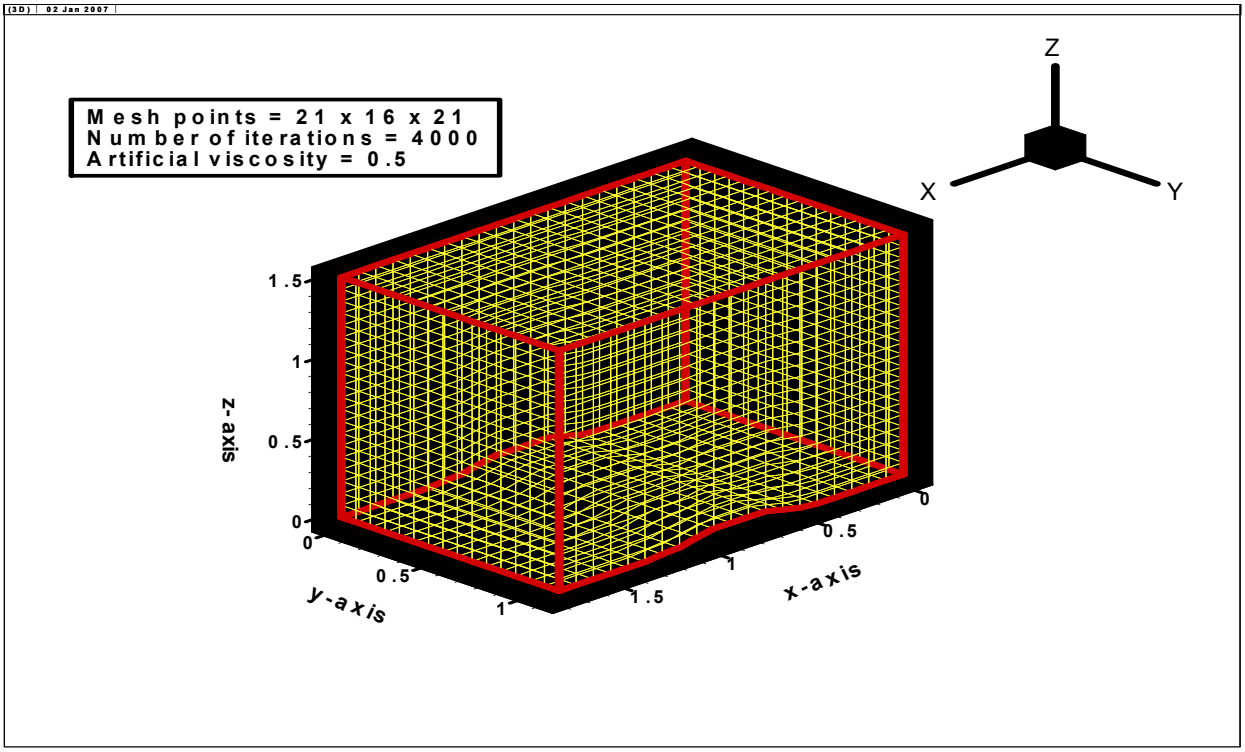

Fig.(1): Algebraic grid generation over a three -dimensional arc circular bump with mesh points (21 x 16 x 21)

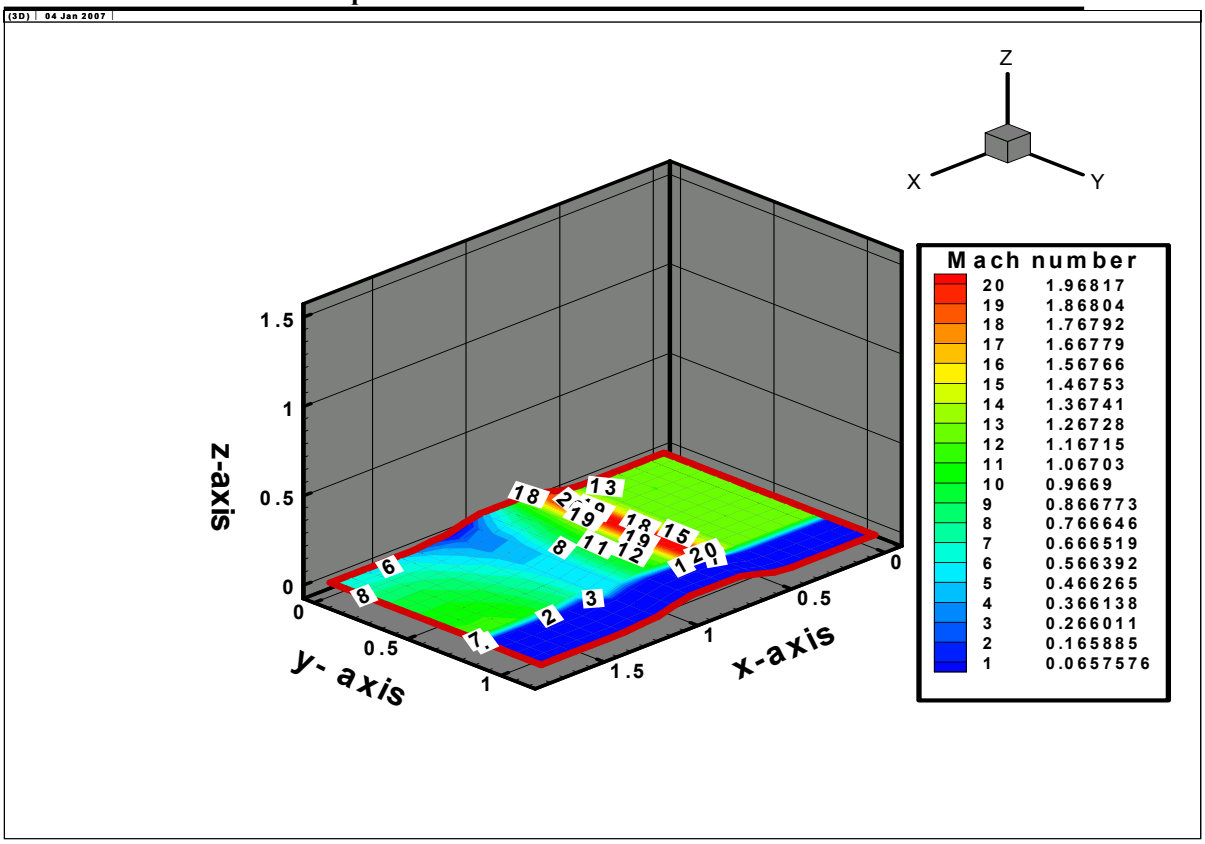

Fig.(2): Mach number contours over a three-dimensional arc circular bump at free stream Mach number = 1.97

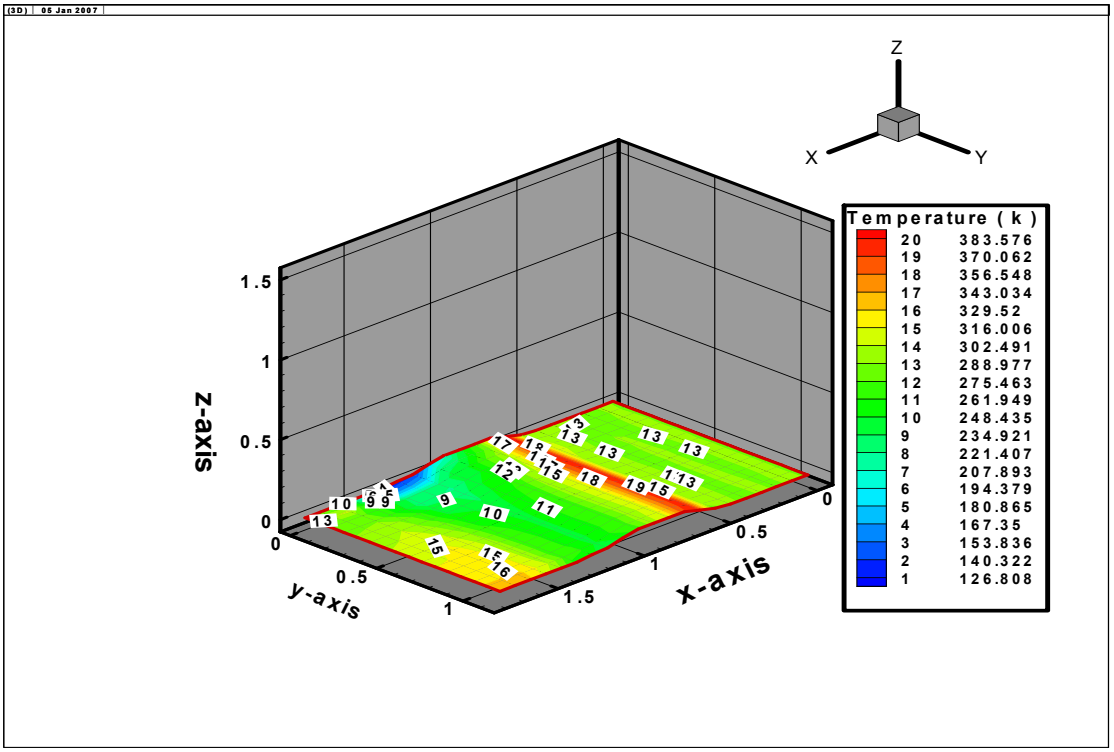

Fig.(3):Temperature contours over a three -dimensional arc circular bump for free stream Mach number = 1.97

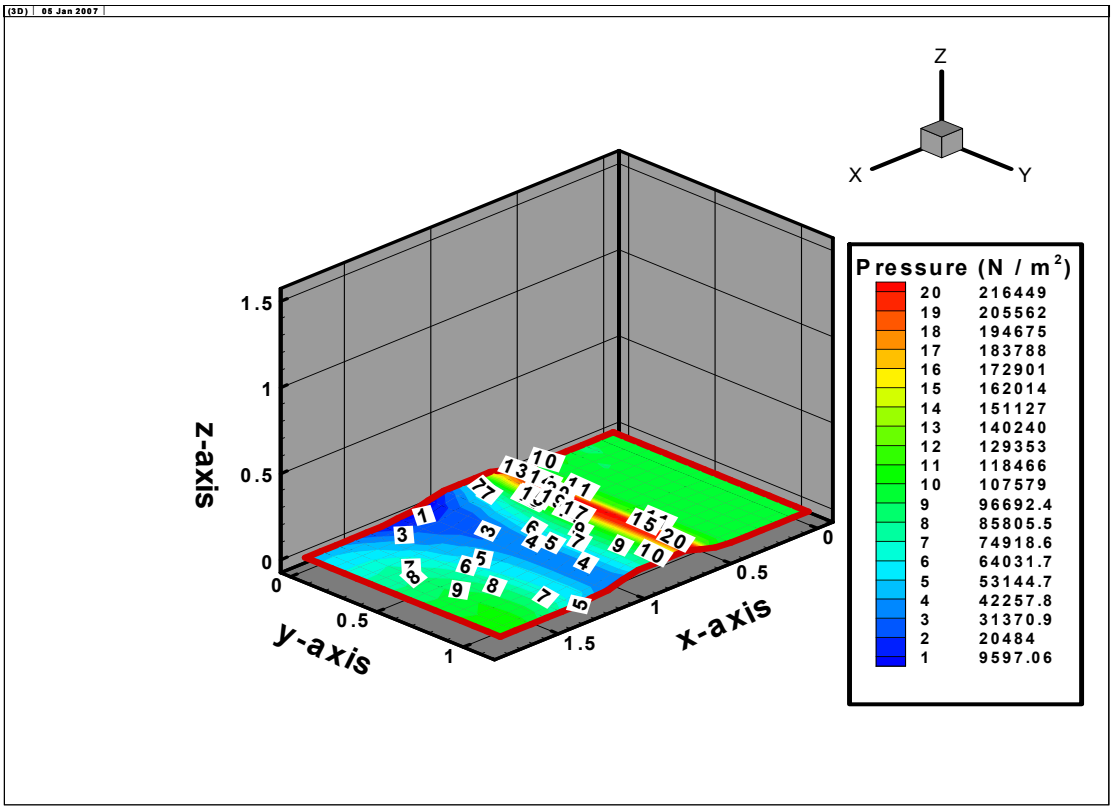

Fig.(4):Pressure contours over a three -dimensional arc circular bump for free stream Mach number = 1.97

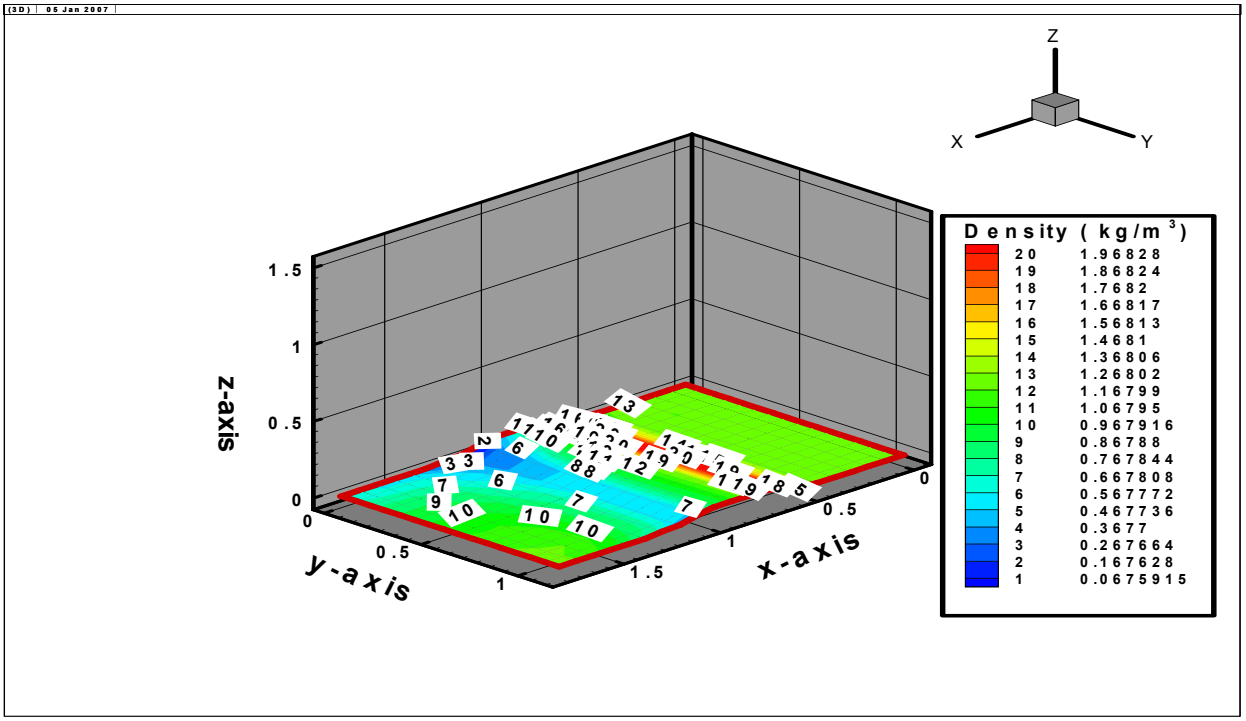

Fig.(5): Density contours over a three- dimensional arc circular bump for free stream Mach number = 1.97

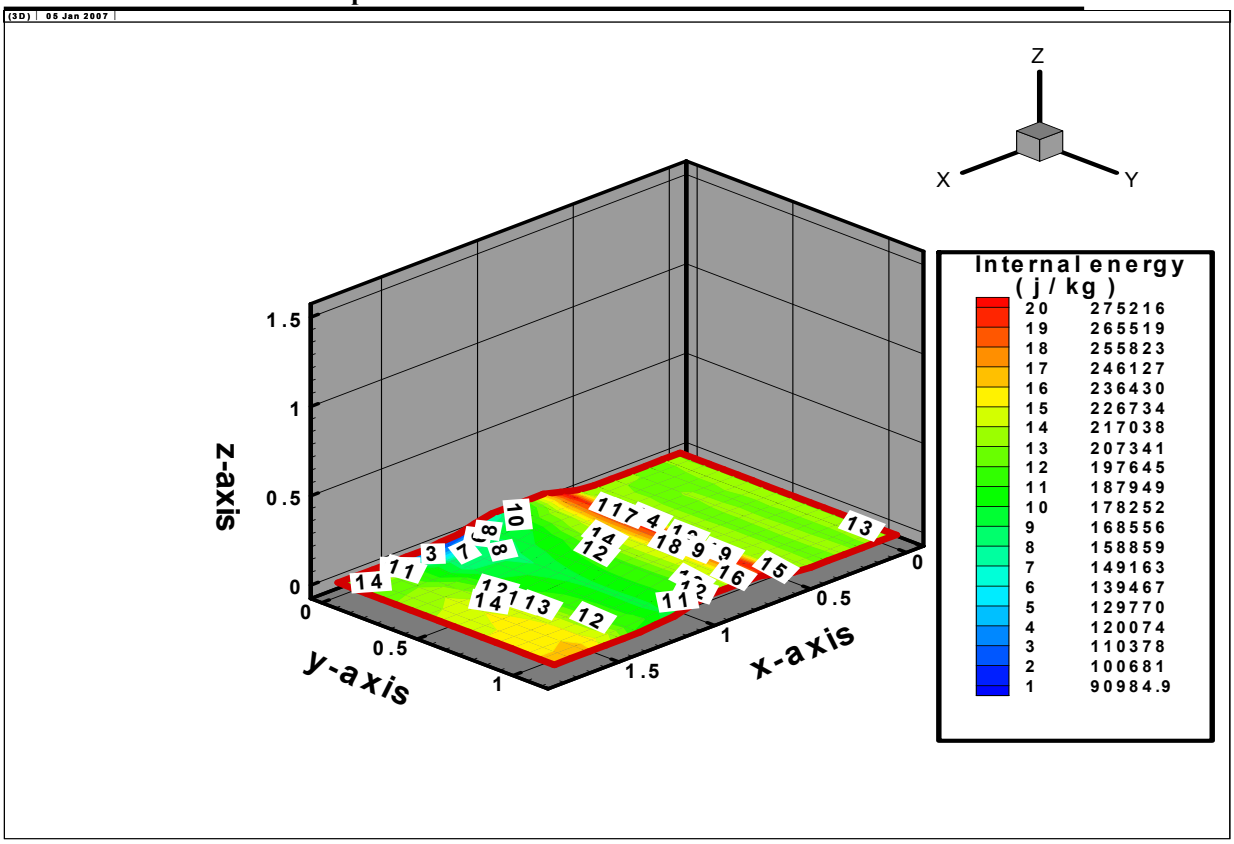

Fig.(6):Internal energy contours over a three dimensional arc circular bump for free stream Mach number = 1.97

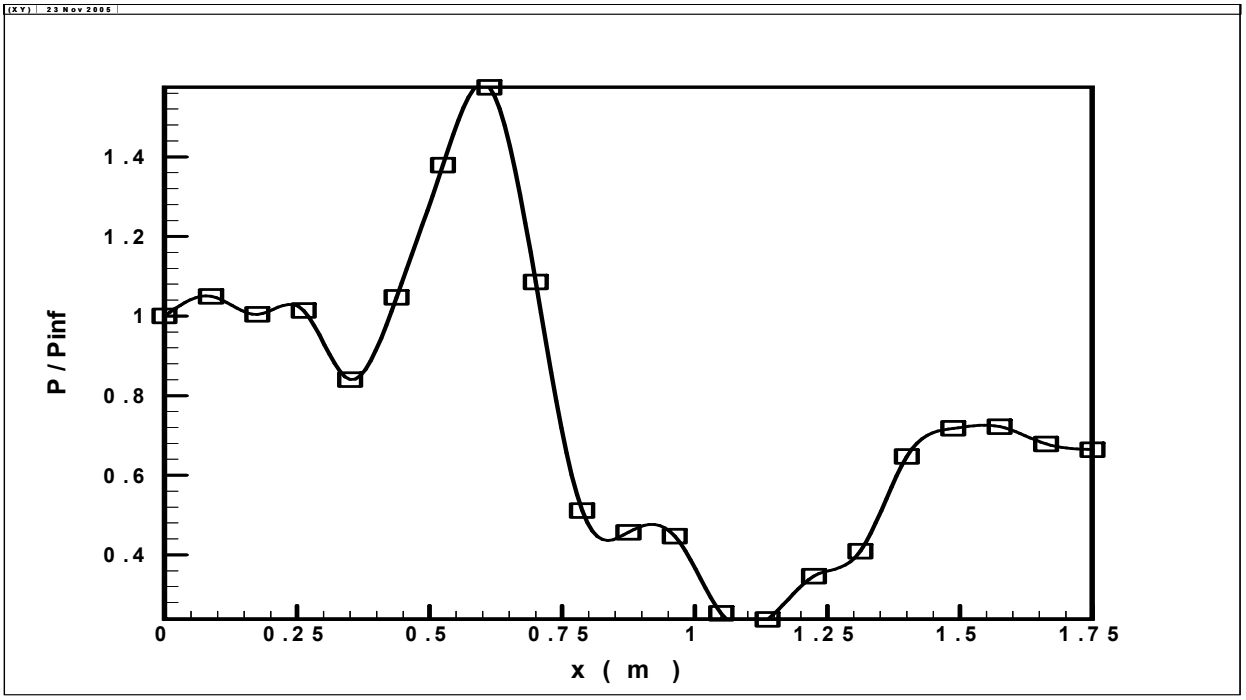

Fig.(7): Wall pressure ratio profile along a three-dimensional arc circular bump for free stream Mach number = 1.97

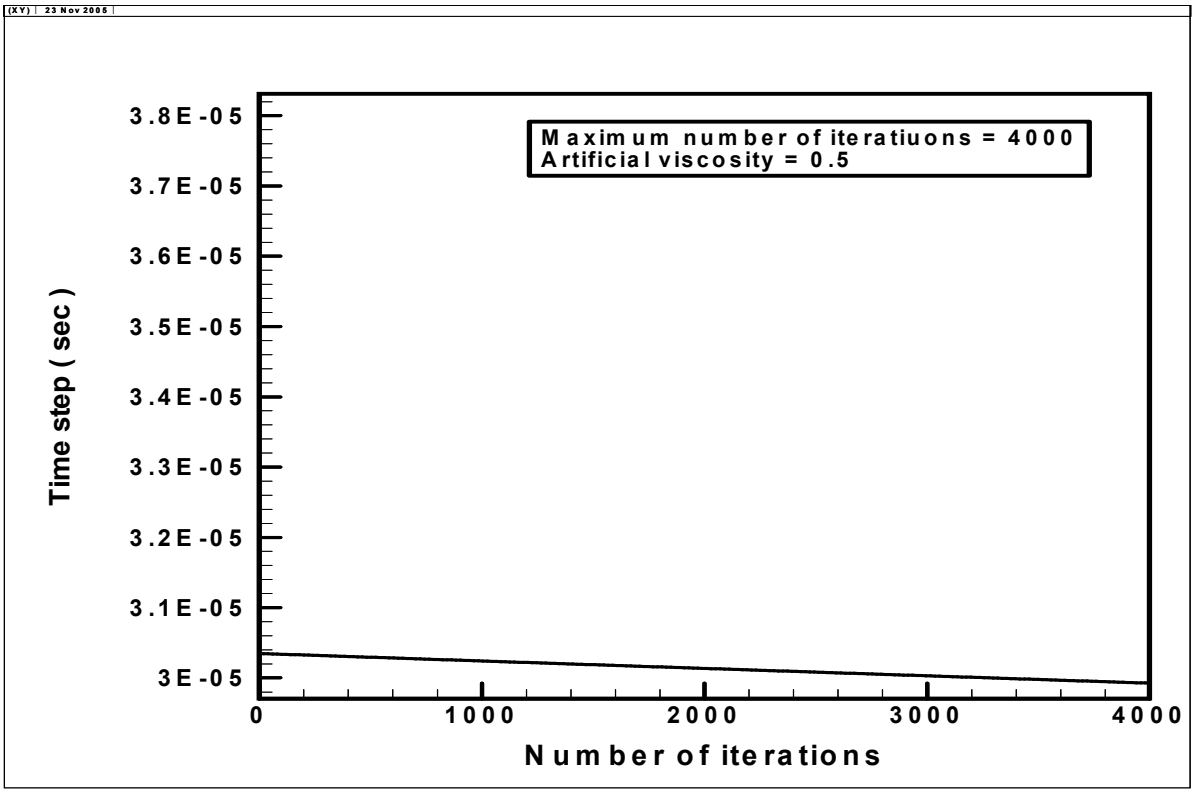

Fig.(8): Historical convergence of supersonic flow past a three-dimensional arc circular bump at free stream Mach number = 1.97

REFERENCES

AL-Dulaimy, F.M., "Numerical Prediction of Supersonic Inviscid and Viscous Flow over Arbitrary Configurations", Ph.D. thesis, University of Technology, Baghdad , 2002.

Anderson , J.D. ," Computational Fluid Dynamics **,** The Basic with Applications ",McGraw-Hill Book Company , U.S.A., 1995.

Dietz ,W. , Wang ,L., Wenren ,Y., Caradonna , F. and Steinhoff , J. ,"The Development of a CFD-Based Model of Dynamic Stall ",American Helicopter Society , 60th Annual Forum , Baltimore , U.S.A. , 2004, pp 1-17.

Fox, M. "Supersonic Aerodynamic Characteristic of an Advanced F-16 Derivative Aircraft Configuration ", NASA Technical Paper 93-3355 , 1993, pp:: 1-22.

Hoffmann,A.K.,"Computational Fluid Dynamics for Enginering ", University of Texsas, 1989.

Hosseini, R. ,Rahimian ,M. and Mirzaei ,M.," Performance of High-Accuracy Schemes in Inviscid Fluxes Calculation " ,Unpublished paper, By e-mail from : hoseinis @ me.ut.ac.ir.

Marsden,O.,Bogey,C.and Bailly ,C.," Higher-Order Curvilinear Simulations of Flows around Non-Cartesian Bodies",AIAA paper 2004-2813,2004,pp1-15.

Sorensen , N., "3D Background Aerodynamics Using CFD", Riso National Laboratory Publications,Roskilde , Denmark ,2002**,** pp 1-18.

Wylie,C.R.,"Advanced Engineering Mathematics", International Student Edition , MacGraw -Hill Book Company,U.S.A.,1966.

Nomenclature

Symbole	Description
a	Speed of sound. m/s
CFL	Courant Fridrich Lewys stability condition.
C_ξ, C_ζ, C_η	Artificial viscosity coefficients in ξ, ζ and η directions respectively.
e	Specific internal energy per unit mass. J/kg
E_t	Total energy per unit volume. J/m^3
E,F,G	Column vector in Cartesian coordinates.
$\overline{E}, \overline{F}, \overline{G}$	Column vector in body fitted coordinates.
L	Length of the arc circular bump. m
J	Jacobian of coordinates transformation.
M_∞	Free stream Mach number.
P_∞	Free stream pressure. N/m^2
$\underline{Q}$	Flux vector.
$\overline{Q}$	Vector of conserved variable in body fitted coordinates.
Re	Reynold's number.
R	Universal gas constant. J/ kg. K
SQ_1	Artificial viscosity term.
T_∞	Free stream temperature. K
t	Time. s
u	Velocity component in x-direction. m/s
U	Contravariant velocity component in ξ-direction m/s
v	Velocity component in y-direction. m/s
V	Contravariant velocity component in η-direction m/s
w	Velocity component in z-direction m/s
W	Contravariant velocity component in ζ-direction m/s
x , y, z	Cartesian coordinates. m/s